



Experimental investigation on the influence of passive/active pre-chamber injection strategy on the hydrogen knock limit

ARTICLE INFO

Received: 9 May 2025 Revised: 29 May 2025 Accepted: 20 June 2025 Available online: 7 July 2025 Hydrogen combustion in an engine is related to the high speed of the process, the wide variability of the excess air ratio, and the high intensity of knock combustion. This paper presents analyses of knock combustion in a TJI engine under passive and active pre-chamber fuelling. The tests were conducted on a single-cylinder AVL 5804 test engine at n=1500 rpm and medium load (IMEP = 3-4 bar). Attention was focused on the knock indicator – MAPO at different excess air ratio values. The possibilities of reducing this phenomenon in the TJI engine during different pre-chamber fuel injection strategies and at different excess air ratio values are presented. The probability of knock occurrence was determined cycle by cycle for several combustion cases (including a further 2 to 5 engine cycles). The paper shows that knock occurs differently in the main chamber and pre-chamber when the engine is actively or passively fed.

Key words: hydrogen engine, TJI combustion system, active and passive pre-chamber, knock intensity

This is an open access article under the CC BY license (http://creativecommons.org/licenses/by/4.0/)

1. Introduction

1.1. Carbon and carbon-free fuels

The search for substitutes for fossil fuels leads to a reduction in greenhouse gas emissions (mainly CO_2), while at the same time increasing the conversion efficiency of energy sources. Hydrogen as a fuel for transport is used in fuel cells (high-purity hydrogen – 99.97% according to ISO 14687:2025, ISO 19880-8:2024, and ISO 19880-9:2024) and in internal combustion engines (hydrogen with limited purity) in the form of a single-component fuel or multicomponent fuel. Dual-fuel systems mainly involve the co-combustion of hydrogen with the following fuels:

- petrol, LPG, ethanol
- natural gas or in the form of HCNG (methane, H₂-CNG blend)
- diesel
- ammonia.

1.2. Turbulent Jet Ignition combustion system

An interesting way of burning hydrogen in combination with the above-mentioned fuels is to use a two-stage Turbulent Jet Ignition system. An engine equipped with such a system is characterised by having two combustion chambers. A pre-chamber and a main chamber. The prechamber usually does not exceed 5% of the volume of the main chamber [20]. Ignition takes place in the prechamber, then flames enter the main chamber through the prechamber orifices to ignite the remaining fuel-air mixture there. The TJI ignition system is divided into two types, with an active prechamber and a passive prechamber. The passive prechamber is filled during the compression stroke with homogeneous fuel-air mixtures available in the main chamber. The active pre-chamber system is integrated with an auxiliary fuel-metering device to accurately control the equivalence ratio of the stratified mixture [27]. The influence of the prechamber design (number and diameter of holes) on the combustion process was investigated by Wakasugi et al. [24]. The results of the research showed that a small number of orifices was advantageous for getting longer penetration into the main chamber. The number of orifices hardly affects the cone angle of the torch flame. The study also shows that the cone angle is consistently larger for larger orifices diameter. Excessively high jet velocity at a smallsized nozzle increases flame stretching and cooling losses at the orifice hole. The effect of pre-chamber orifices diameter on combustion parameters in a hydrogen-fuelled TJI engine was also analysed by Górzyńska et al. [6]. The research was a numerical simulation using CFD analysis of the combustion process inside the prechamber and main chamber. The study showed that increasing the diameter of the holes led to an increase in the maximum pressure in the cylinder and the rate of heat release. An important conclusion of the study is also that the maximum temperature value in the cylinder increased with the increase in the diameter of the holes. The presented properties of the TJI ignition system mean that it has the potential to be used during the combustion of dual fuels, especially in the case of an active prechamber.

1.3. Co-combustion of hydrogen with other fuels

The combustion of pure hydrogen is usually carried out using indirect injection (PFI) or direct injection (DI). An analysis of direct injection of hydrogen into an engine was presented by Liu et al. [11]. The central hydrogen injection at medium load (10 bar) and 1500 rpm without exhaust gas recirculation was used. The maximum indicated combustion efficiency was obtained at 45% with four injector orifices.

Research carried out by Gürbüz et al. [9] involved the use of a two-stage combustion system during the combustion of hydrogen with petrol. Hydrogen was injected into the intake manifold, and petrol was injected into the prechamber (it accounted for about 2% of the total volume). Tests were carried out with varying values of λ (0.8–1.2) at n=2300 rpm. Increasing the excess air ratio results in an

extension of the combustion duration in the range of 0–10% mass fraction burned (MFB) with a corresponding increase in the fuel dose to the pre-chamber. Increasing the dose to the prechamber at different excess air ratios led to settling of the load at 6.3 bar. At lower values of λ a higher load was observed (about 6.6 bar), at $\lambda = 1.2$ the IMEP value equaled 5.1 bar. The unevenness of the combustion process (as determined by CoV(IMEP)) was greatest when using the passive combustion chamber and increased from 0.8% to 3.0% when increasing the excess air ratio.

The study by Shi et al. [19] was conducted on a TJI engine at a relatively high compression ratio (17.5:1), excess air ratio $\lambda = 2.1$, and n = 3000 rpm. The pre-chamber was fuelled with hydrogen, and the main chamber with gasoline. This fuel injection strategy resulted in low NO_x concentrations (approximately 20–30 ppm) being recorded at 1–2 MPa hydrogen injection pressure. This value increases with the advance of the ignition angle.

Vehicle simulation studies (AVL Cruise) performed by Rimkus et al. [17] show that a small addition of hydrogen (5%) to petrol results in a large increase in nitrogen oxides concentration (by about 20%) during the WLTC test. The addition of hydrogen also resulted in a reduction of other gaseous components: CO by 22%, CO₂ by 15% and hydrocarbons by more than 35%.

The combustion of diesel fuel with additions of hydrogen and natural gas was studied by Menaa et al. [13] in the research, a dual-fuel (diesel-natural gas) was used with various hydrogen additions (from 0 to 20% H₂). The lack of natural gas addition in the fuel resulted in a higher maximum thermal efficiency of the engine (30%) than the system with natural gas addition. In the second case, only at maximum load was greater efficiency achieved (around 32%).

Yang et al. [26] investigated the effect of varying hydrogen content in the pre-chamber, while feeding the main chamber with methane, on engine performance. Feeding the pre-chamber with hydrogen resulted in an increase in thermal efficiency of up to 46% (with a passive chamber, the result was about 45%). The use of the passive pre-chamber also resulted in an increase in nitrogen oxide emissions of approximately 70%. Fueling the pre-chamber with methane or hydrogen rapidly reduced NO_x emissions. (at $\lambda = 2.0-2.1$).

Combined combustion of hydrogen and ammonia (despite much worse thermodynamic performance) is becoming more and more important. Research by Guo et al. [8] conducted with a TJI engine involved feeding the main chamber with NH₃ + H₂ and pre-chamber with H₂ at $\lambda = 1$ (in the main chamber). With an increase in the hydrogen blending ratio from 10% to 50%, the ammonia combustion efficiency improves from 96.9% to 98.6%, accompanied by a significant reduction in the unburned ammonia emissions.

A simulation study of the combustion of hydrogen with ammonia was conducted by Zue et al. [28]. Analyses were conducted with direct mixture injection ($\lambda = 2.0{\text -}3.0$) in the range of 10–30% ammonia content. A higher value of the excess air ratio increases the combustion duration while sharply reducing IMEP. The highest thermal efficiency (47.5%) was obtained at 20% NH₃ and $\lambda = 2.5$ (increase or decrease of λ resulted in a deterioration of efficiency).

Consideration of the use of hydrogen in combination with conventional and alternative fuels shows that its high reactivity can bring benefits in terms of thermal efficiency. Hydrogen as a carbon-free fuel may also prove to be a way of reducing emissions of harmful carbon compounds such as unburned hydrocarbons, CO₂ and CO. An engine with a TJI ignition system is a promising way to use hydrogen together with previously mentioned fuels, but it is important to first investigate the effects of TJI engine operating conditions on knocking combustion during hydrogen combustion.

1.4. Knock during combustion of hydrogen

Knock combustion is assumed to be incorrect combustion of air-fuel mixture resulting in the generation of uncontrolled pressure waves acting against the main combustion source leading to a decrease in overall engine efficiency [12]. For conventional liquid fuels, an octane number is determined which indicates the resistance of the fuel to knocking combustion. The octane number scale is determined by comparing fuels with two standards, heptane, which has an octane value of 0, and iso-octane, which has an octane value of 100. In the case of liquid hydrogen, a laboratory octane number in excess of 130 has been recorded, meaning that in this form it has a high resistance to knocking. However, it is noteworthy that for the methane number used for gaseous fuels, hydrogen is used as a standard, which has a 0 on this scale, meaning that in its gaseous state of matter it is a fuel susceptible to knock combustion [23]. Hydrogen as a fuel has a wide flammability range $(\lambda = 0.14-10)$, a low minimum ignition energy (0.017 mJ), and a high laminar combustion rate (2.91 m/s) [2, 4, 5]. However, the process of hydrogen combustion in an internal combustion engine generates some problems, and the main reason for that is the dual nature of hydrogen knock. It consists of two mechanisms, heavy and light knock. The first one is described as air-fuel autoignition at the end of the combustion stroke caused by high temperature and pressure in the combustion chamber. Light knock is the unstable combustion of an ignited air-fuel mixture initiated by a controlled source of combustion [12]. Investigating the range of occurrence and intensity of knocking combustion during hydrogen combustion in a TJI engine with active and passive injection modes is an important element in considering it use as a fuel.

2. Materials and methods

2.1. Test bench

The pre-chamber injection strategy was examined using a single-cylinder AVL 5804 research engine. The technical data are shown in Table 1. The engine was equipped with a pre-chamber with a volume of $V_{PC}=2.1~{\rm cm}^3$ and 6 orifices with a mean diameter of 1.7 mm. The engine was fed with hydrogen in two variants: with a passive pre-chamber (without fuel supply to the PC), with an active pre-chamber (with fuel supply to the PC).

The engine is equipped with an 8-channel AVL IndiSmart high-speed measurement system. The test bench includes flow meters for intake air (Sensyflow ABB), hydrogen in the main chamber (Bronkhorst 111AC-70K), and hydrogen in the pre-chamber (Bronkhorst 111B-100).

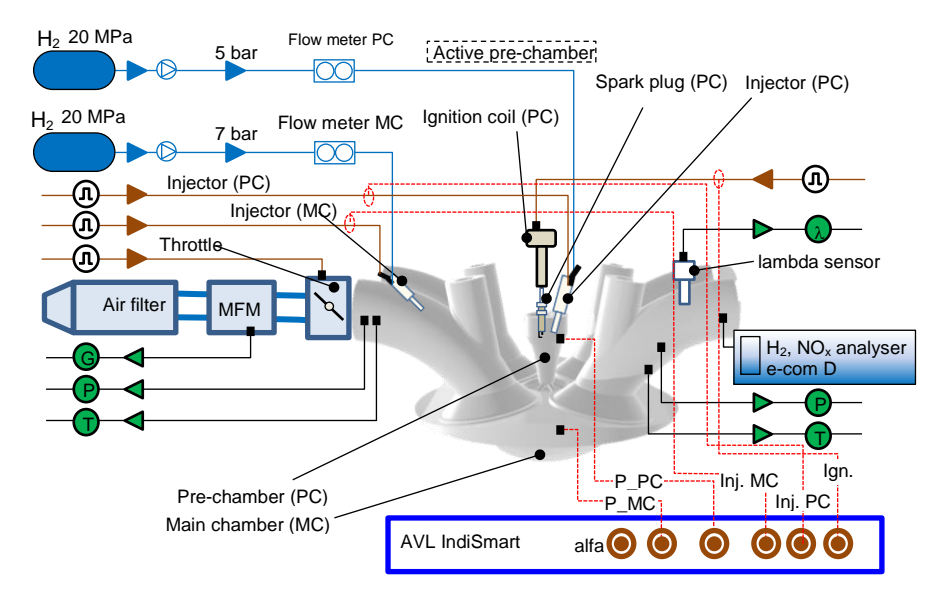


Fig. 1. Schematic diagram of the test bench for hydrogen combustion in a two-stage combustion system (with an active or passive pre-chamber)

A broadband LSU 4.9 lambda sensor was used to measure the oxygen content in the exhaust gases. Along with the LSU 4.9 sensor, an LCP80 controller, adapted for oxygen measurement during hydrogen fueling, was employed. The ECU Master EMU Black system was used to control the electronic throttle and ignition timing. Basic information on the control and measurement equipment is provided in Table 2.

Table 1. Engine specification

Engine type	AVL 5804; 4-valve; TJI, passive, active	
	pre-chamber	
Bore × stroke	85 × 90 mm	
Compression ratio	14.5:1	
Pre-chamber volume	2.1 cm ³	
Main chamber volume	510 cm ³	

Table 2. Measurement equipment used during the knock combustion experiment

Equipment	Producer, measurement range	Resolution
Air flow meter	ABB SensyFlow 0–720 kg/h	error < ±0.8%
Fuel flow meter PC	Bronkhorst 111B-100 0.16–25 ln/min	±0.1% FS
Fuel flow meter MC	Bronkhorst 111AC-70K 0.4–100 ln/min	±0.1% FS
Acquisition system	AVL IndiSmart; 8-channels	0.1 deg
Pressure sensor PC	Kistler M3.5 6081 AQ22	0–25 MPa
Pressure sensor MC	AVL GH14D	0–25 MPa
Inlet air temp.	Linuatherm Pt 100	−30−180°C
Inlet air pressure	Wika A-10	0–10 bar
Exhaust temperature	Czaki K thermocouple	0-1000°C
Exhaust pressure	Wika A-10	0–10 bar
Lambda sensor	LSU $4.9 + LCP 80$ $\lambda = 0.7 \text{ to } 12.5$	0.1
Injection control system	Mechatronika	0–20 ms, ±0.1 ms
Ignition control system	ECU Master EMU Black	0.5 deg
Throttle control system	Bosch ETB 32 mm 0–90 deg	1 deg

High-speed measurements were carried out during the analysis of 100 consecutive engine cycles. Measurements were taken of the combustion pressure in both engine chambers, the ignition point, fuel injection into the intake manifold, and the pre-chamber. In addition, the excess air ratio, throttle position, pressure, and temperature in the engine intake and exhaust systems were recorded.

2.2. Scope of the research

The research work aimed to analyse hydrogen combustion in an engine with a two-stage combustion system, focusing on knock combustion. For both combustion cases (passive, active), the ranges of the knock combustion defined by the MAPO coefficient were determined. The full scope of the research work is shown in Table 3.

Table 3. Scope of work on knock combustion of the TJI engine $\,$

Passive pre-chamber		
λ	1.25; 1.35; 1.50; 1.60; 2.00	
СоС	var; 2 deg; each successive one was due to an increase in ignition delay	
Ignition	regulated, CoC-dependent	
IMEP	3.5–4.0 bar	
n	1500 rpm (const)	
Active prechamber		
λ	1.6; 2.0; 2.5; 3.0	
СоС	2 deg; each successive one was due to an	
	increase in $\Delta qo_PC = 2 \text{ ms}$	
Ignition	const	
IMEP	3.5–4.0 bar	
n	1500 rpm (const)	
MC injection control strategy qo_MC	mode: const;	
	mass flow: 166.7 g/h	
	injection time: 7 ms	
	injection pressure: 7 bar	
	fuel dose: 3.76 mg/inj	
	fuel dose energy: 450 j/inj	
MC injection control strategies qo_PC	mode: var	
	mass flow: 0–10 g/h	
	injection time: $0-10 \text{ ms } (\Delta t = 2 \text{ ms})$	
	injection pressure: 5 bar	
	fuel dose: 0–0.23 mg/inj	
	fuel dose energy: 0–28 J/inj	

Hydrogen combustion in the passive combustion system was achieved by adjusting the ignition timing to obtain a 2-degree delay in the Center of Combustion (CoC). In this manner, measurements were taken from CoC = 2 deg to CoC = 18 deg aTDC. The excess air ratio was kept constant.

Hydrogen combustion in the active mode was carried out with a constant ignition timing and a simultaneous increase of the fuel dose to the pre-chamber. The amount of fuel dose to the main chamber was constant. Increasing the amount of fuel injected into the pre-chamber accelerated the combustion centre towards TDC, for which reason the dose was reduced at several test points. Increasing the dose to the pre-chamber resulted in a change in the magnitude of the global excess air ratio, which varies in the range where knock combustion occurs. This range of global excess ratio was also taken into account in the results of the study.

2.3. Methodology for interpreting knock combustion

MAPO (maximum amplitude of pressure oscillation) is the most commonly used evaluation indicator in knock tests [3, 10]. It indicates the intensity of the impact generated by the abnormal combustion:

$$MAPO = \frac{1}{N} \sum_{1}^{N} max_{IGN,IGN+KN} |\tilde{p}|$$
 (1)

where N- number of cycles, $|\tilde{p}|-$ filtered cylinder pressure (explained further), IGN - ignition angle, KN - duration of knock combustion.

As MAPO increases, the tendency and intensity of knock combustion rise. There is currently no clear MAPO value that indicates knock combustion. The threshold level depends on the type of engine [3, 10]. The magnitude of the limit has been defined differently: Szwaja and Naber [22] set the value of the knock combustion border at 1 bar. The same value is used by many authors in their studies [14, 21, 25]. Aramburu et al. [1] used a knock combustion limit of MAPO = 4 bar in their study on a 6-cylinder engine with a displacement of 5883 cm³. The same MAPO limit was used by Pla et al. [15], despite the fact that the displacement of the indirectinjection engine was only 1300 cm³. For engines with a large displacement (5 dm³/cyl.), the MAPO value was increased to 5

bar [7]. Otherwise, the parameter depended on the filter size. Puzinauskas [16] highlighted two ranges: 4–9 kHz, with MAPO limit = 0.15 bar, and at 4–12 kHz, with MAPO limit = 0.23 bar. Shi et al. [18] attempted to correlate MAPO with the maximum value of average luminance, achieving an R-squared fitting value of 0.67. This indicates that MAPO follows a moderate exponential relationship with the peak average flame brightness, and that greater knock resistance results in a higher peak average flame intensity brightness.

The knock combustion analysis was carried out according to the scheme shown in Fig. 2. The cylinder pressure curve recorded during the combustion process (1) was digitally filtered at 4 kHz. Then, deviations from the mean value within the 4–20 kHz range were extracted in the form of MAPOx (2). Positive and negative oscillations were presented as absolute values – PP (3). Based on this, the maximum oscillation changes – PPmx – were determined for each cycle (from the 100 cycles analyzed – (4)).

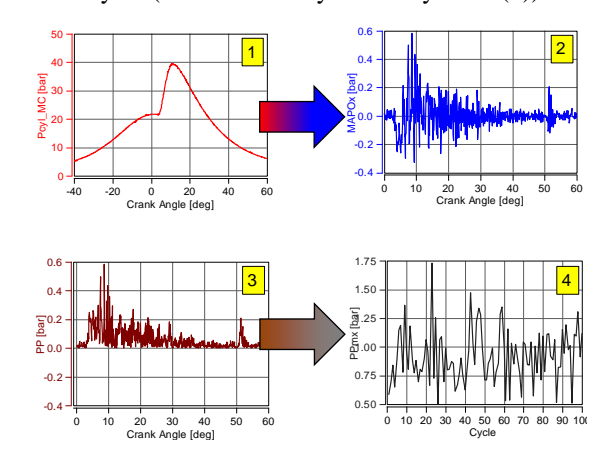


Fig. 2. Calculation process of MAPO

3. Results and discussion

3.1. Combustion with passive pre-chamber

The combustion process was analysed at different values of λ and varying CoC settings. Pressure changes in both chambers are shown in Fig. 3.

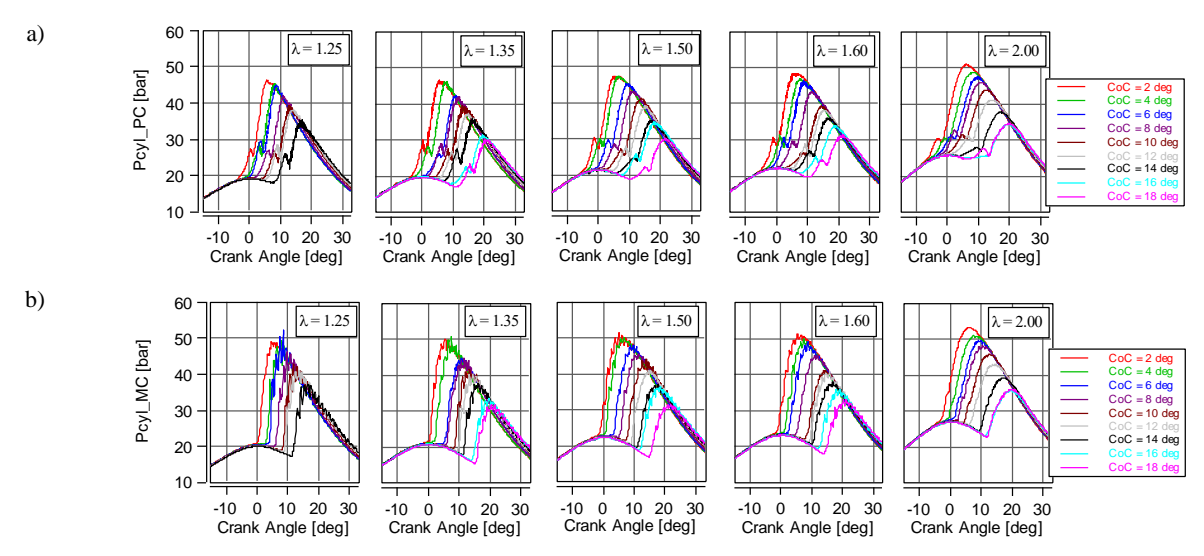


Fig. 3. Combustion pressure: a) in the pre-chamber PC; b) in the main chamber MC, at different CoC values at n = 1500 rpm; $\lambda = 1.25$, passive pre-chamber

The initiation of the combustion process in the prechamber (Fig. 3a) occurs near TDC. Then flames from the pre-chamber enter the main chamber, thereby igniting the fuel-air mixture. Significant pressure oscillations are observed in the main chamber, which are indicative of knock combustion (Fig. 3b). An analysis of the operating point $\lambda=1.25$ with varying CoC is shown in Fig. 3a. The occurrence of knock combustion is visible at each CoC value. Even a significant ignition delay (CoC = 14 deg aTDC) indicates the presence of knock combustion.

3.2. Combustion with active pre-chamber

36

Figure 4 shows the pressure in the cylinder (main chamber) during use of the active pre-chamber with variable λ and changing fuel dose to the pre-chamber. Increasing the fuel injection to the PC (Fig. 4a) results in a reduction

of λ with a simultaneous rise in combustion pressure at the PC and MC (Fig. 4b). At the same time, an enhancement of the pressure peak responsible for ignition in the prechamber is observed.

The absence of fuel injection into the pre-chamber causes combustion to deteriorate at low λ , although the process can still occur. For a lean air-fuel mixture and no injection into the pre-chamber, a lack of combustion is observed.

3.3. Knock combustion analysis during passive pre-chamber use

To obtain the MAPO magnitude (equation 1), a digital filtering process was performed on the cylinder pressure signal (at f=4 kHz, in the angular range 0–70 deg with pressure signal resolution $\Delta\alpha=0.1$ deg). The results of the high-pass filter were used for further analyses.

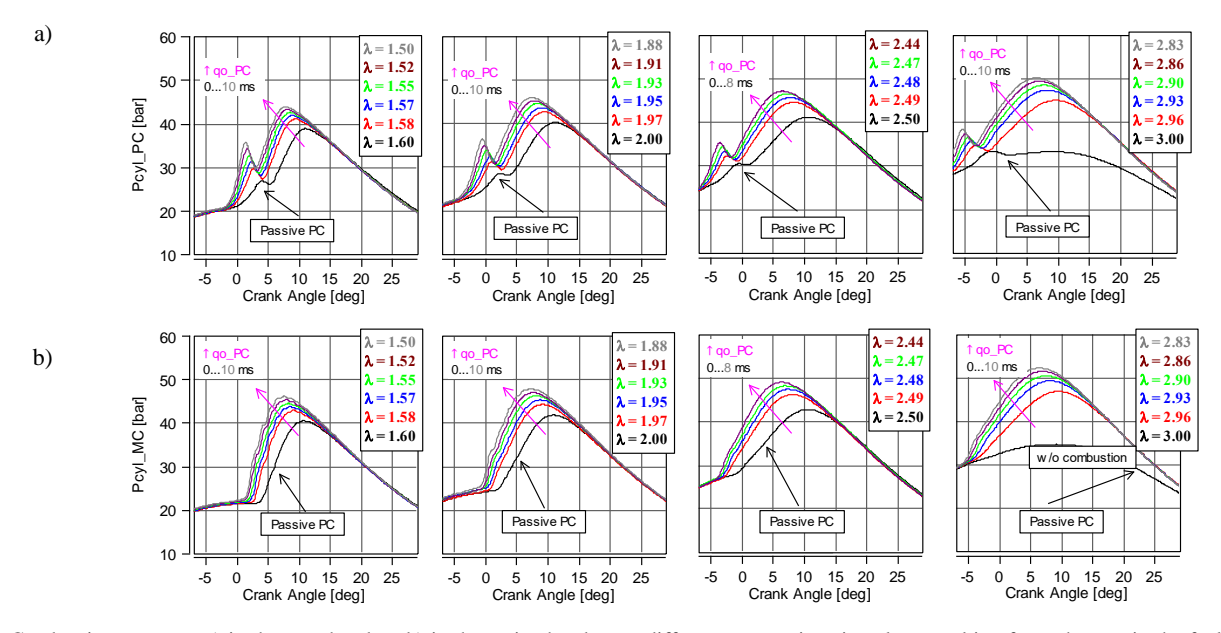


Fig. 4. Combustion pressure: a) in the pre-chamber; b) in the main chamber, at different excess air ratio values resulting from changes in the fuel dose supplied to the pre-chamber at n = 1500 rpm; active pre-chamber; each graph shows the basic excess air ratio and the adjusted excess air ratio (coloured), which change as the changes of fuel dose in pre-chamber ($\Delta t = 2$ ms)

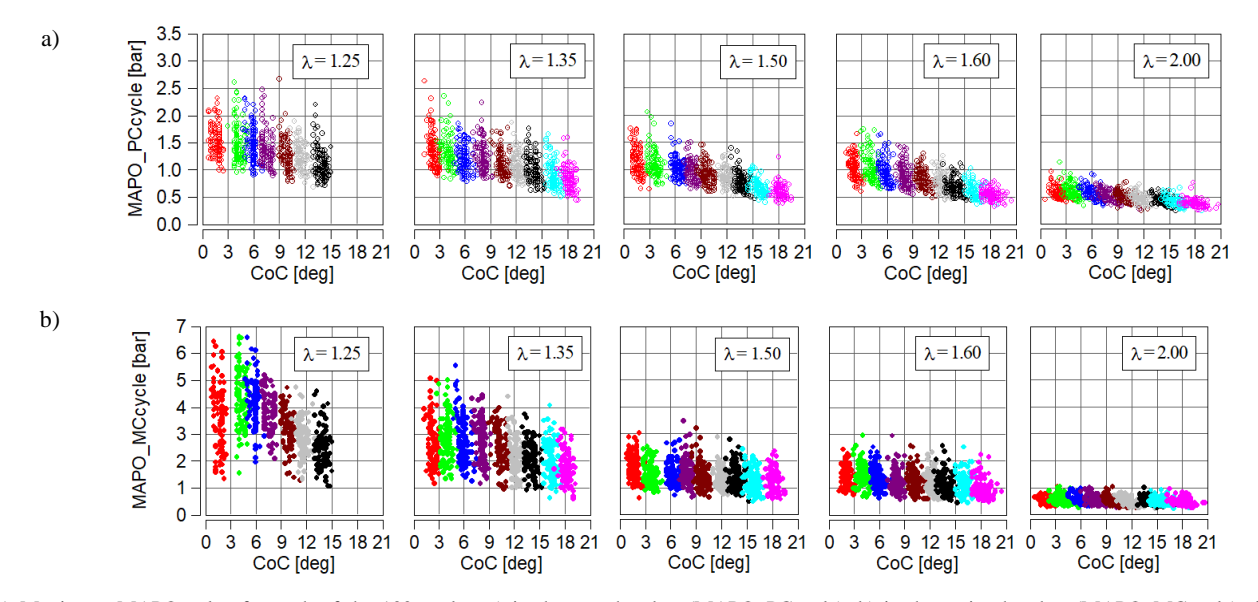


Fig. 5. Maximum MAPO value for each of the 100 cycles: a) in the pre-chamber (MAPO_PCcycle), b) in the main chamber (MAPO_MCcycle), for different CoC and various excess air ratios (passive pre-chamber)

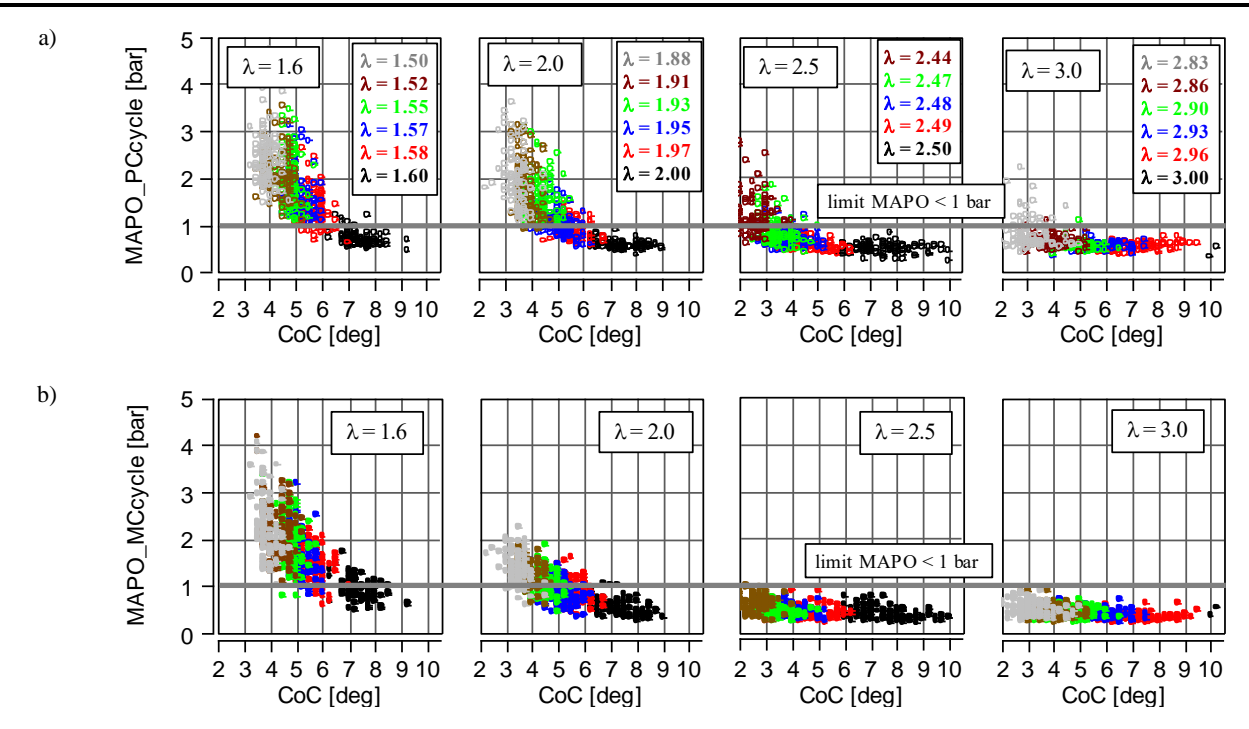


Fig. 6. Maximum MAPO value for each of the 100 cycles: a) in the pre-chamber (MAPO_PCcycle), b) in the main chamber (MAPO_MCcycle), for different CoC and various excess air ratios (active pre-chamber). Each graph shows the basic excess air ratio and the adjusted excess air ratio (colored), which change as the changes of fuel dose in the pre-chamber ($\Delta t = 2 \text{ ms}$)

During the combustion pressure analysis, it was observed that MAPO reaches lower values in the pre-chamber (Fig. 5a) than in the main chamber (Fig. 5b). The study used a passive pre-chamber, so the amount of fuel was not regulated directly inside this chamber. The amount of fuel in the pre-chamber was determined only by the global value of λ obtained by injecting fuel into the intake of the engine. A reduction in pressure oscillations has been achieved in the pre-chamber compared to the main chamber. The absolute maximum values of MAPO_PC relative to MAPO_MC are more than doubled in the range of $\lambda < 1.5$. At higher values of λ these changes are smaller and at $\lambda = 2.0$ the maxima are the same.

In the following section, a full MAPO_MC analysis was carried out for each engine cycle at $\lambda = \text{var}$ and CoC = var (Fig. 5a). Figure 5b shows that increasing the excess air ratio reduces knock combustion. In addition, in the range of each value of λ , increasing the CoC also limits the maximum oscillation of the combustion pressure. It is worth noting that when knock combustion occurs during hydrogen combustion, it is more effective to temporarily reduce the excess air ratio than to delay its ignition (or CoC).

As mentioned earlier, the papers [21, 22, 25] assume that the MAPO limits indicating the occurrence of knock are MAPO > 1 bar. Taking the above conclusions into account, it can be stated that in the passive pre-chamber, both normal and abnormal (knock combustion) cycles occurred under all conditions. However, it can be assumed that at $\lambda > 1.5$ and high CoC values, knock combustion in the pre-chamber is almost non-existent. For $\lambda = 2.0$, knock combustion in the pre-chamber did not occur – regardless of the CoC. Analysis of the same conditions in the main chamber (MC) indicates the absence of knock combustion only at $\lambda = 2.0$.

3.4. Knock combustion analysis during active pre-chamber use

The next step of the research was to analyse the identification and evaluation of the intensity of knock combustion in the active pre-chamber and main chamber at different engine operating parameters. Figure 6 shows the calculated MAPO values for PC and MC, respectively.

From the results, it can be concluded that the leaner the mixture is, the lower the tendency for knock combustion to occur. Furthermore, usually knock combustion is more intense in the pre-chamber than in the main chamber. This is particularly evident for $\lambda=2.5$ and $\lambda=3.0$. Moreover, more intensive knock combustion was recorded at lower CoC values, which means that better combustion conditions occur when an active pre-chamber with a higher dose of injected hydrogen is used. In the case of a fuel-air mixture with $\lambda=1.6$, knock combustion occurs in most of the engine operating conditions. When CoC occurs after 7 degrees aTDC, knock combustion no longer occurs in the prechamber, while it continues to occur in the main chamber.

3.5. Average MAPO analysis with passive PC

Analysis of the global MAPO index for both combustion chambers (Fig. 7a) shows significantly higher values in the main chamber than in the pre-chamber. The highest MAPO values of 4.5 (at $\lambda=1.25$) were recorded when CoC = 4 deg aTDC. When increasing the excess air ratio, the MAPO index obtains almost constant values with a tendency to decrease slightly with increasing CoC. When $\lambda=2.0$, the MAPO remains constant at 0.5 bar, indicating the absence of knock combustion.

Analysis of MAPO in the pre-chamber (passive) shows much smaller variations in this indicator. The maximum MAPO is 1.5 bar at $\lambda = 1.25$ (and then decreases to around 1.0 bar). A similar trend of decreasing MAPO is observed when increasing λ .

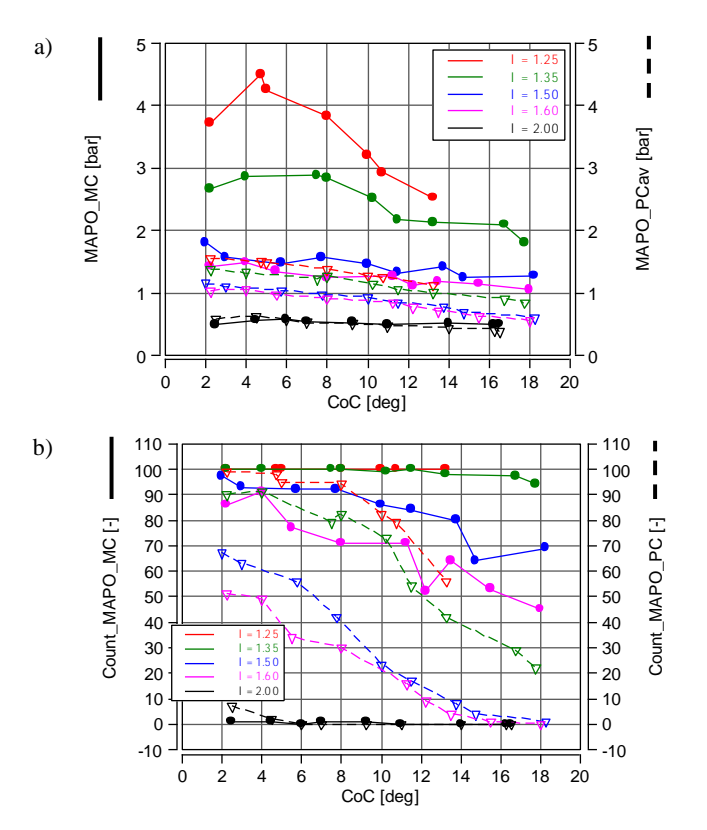


Fig. 7. Knock combustion analysis of the passive chamber: a) average MAPO_MC vs. average MAPO_PC indicators; b) knock combustion occurrence based on threshold values (referenced to 100 analyzed cycles)

Then the number of cycles during which knock combustion occurred (cycles at which MAPO > 1 bar) was counted. With 100 measuring cycles, the percentages correspond to the absolute number of cycles.

The analysis carried out with the AVL Concerto system indicates that at low excess air ratio (λ < 1.5) the number of knock cycles in the main chamber is almost 100% (Fig. 7b). While λ = 1.35 and CoC > 12 deg aTDC, the occurrence of knock decreases slightly and reaches 95%. When λ = 1.5, the highest number of knock cycles occurs at CoC = 2 deg aTDC and equals Count_MAPO_MC = 97%. When λ = 1.6 the number of knock cycles ranges from 86% (CoC = 2 deg aTDC) to 44% (at CoC = 18 deg aTDC). The minimum number of knock combustion cycles was recorded at λ = 2.0: it is only 1% at several operating points, regardless of the CoC.

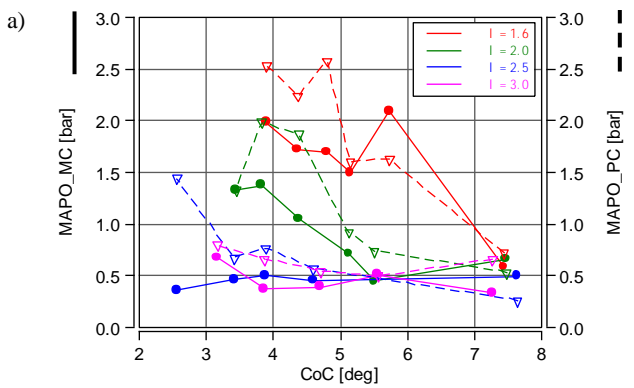
In the pre-chamber, the number of knock combustion cycles was never 100%. At $\lambda=1.25$, the occurrence of knock combustion was 99%. When CoC occurred at 18 deg aTDC the number of knock cycles was 56%. With each higher value λ – the number of knock combustion cycles was lower. When $\lambda=1.5$ and $\lambda=1.6$ the number of knock combustion cycles in the pre-chamber was about 40% less than in the main chamber – and decreased with increasing CoC. When $\lambda=2.0$ in the pre-chamber, only at CoC = 2 deg aTDC and at CoC = 4 deg aTDC, the number of knock

cycles was higher than in the main chamber. For the higher CoC, there was no knock in the pre-chamber during any of the analysed engine cycles.

3.6. Average MAPO analysis with active PC

Controlling the combustion in the active pre-chamber system involved increasing the fuel dose in the PC, which had the effect of reducing CoC. This type of regulation results in an increasing MAPO in the PC and MC while limiting the CoC. For $\lambda=1.6$ and $\lambda=2.0$ MAPO value is well above the 1 bar (Fig. 8a). When combusting a very lean air-fuel mixture ($\lambda=2.5$ and $\lambda=3.0$) MAPO was limited. However, it was always higher in PC than in MC.

An analysis of the number of knock combustion cycles (Fig. 8b) shows the high occurrence of knock combustion when $\lambda \leq 2.0$. A higher number of knock cycles was recorded under these conditions in PC than in MC. When $\lambda = 3.0$ knock combustion is completely eliminated in MC, while it still occurs in PC (at low CoC values).



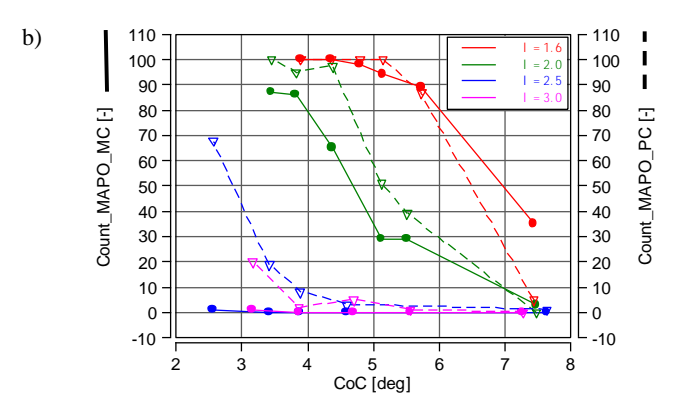


Fig. 8. Knock combustion analysis of the active chamber: a) average MAPO_MC vs. average MAPO_PC indicators; b) number of knock combustion events based on threshold values (referenced to 100 analyzed cycles)

3.7. Assessment of the probability of knock combustion occurrence

The analysis of knock combustion was presented in the previous chapter. An assessment of the occurrence of knock combustion per 100 engine cycles is also included there. The probability of knock combustion occurring cycle-bycycle is analysed below. The following analysis covers knock combustion of two, three, four and five cycles occurring in sequence. This comparison was made for passive and active pre-chamber.

The probability of knock combustion of two cycles occurring in succession was determined as cycle-to-cycle → CTC(2). Similarly, the subsequent values of the 100-cycle combustion were determined cycle-by-cycle.

The probability of cycle-by-cycle knock combustion in the passive chamber was carried out during combustion at $\lambda = 1.25$; 1.35; 1.5 and 1.6. Cycle-by-cycle combustion at $\lambda = 2.0$ was not analysed, because the occurrence of knock in this case was very low (Fig. 7b).

An analysis of the probability of knock combustion at $\lambda=1.25$ shows the virtually continuous occurrence of this phenomenon. The number of knock cycles in the MC was 99, so the probability of abnormal combustion is CTC(2) = 98%. The value for five consecutive knock cycles is CTC(5) = 95%. These values barely change when delaying the occurrence of the combustion centre (Fig. 9a). Analysis of knock combustion in the pre-chamber shows slightly different figures. As the CoC increases, the number of knock combustion cycles decreases. The probability of obtaining 50% of the cycles with CTC(5) combustion does not occur at CoC = 14 deg aTDC. For the remaining (lower CTC values), knocking combustion with a probability of 50% occurs for all other CTC values.

Analysis at $\lambda = 1.35$ reveals that in the main chamber, the change in CTC value is linear (Fig. 9b). In contrast, in the pre-chamber, the CTC(3) value takes on a much lower

probability than CTC(2). A linear decrease in probability is observed during CTC(4) and CTC(5).

During combustion at $\lambda=1.5$, a linear decrease in the probability of successive knock cycles is observed with increasing CoC. A similar trend is also observed in the prechamber. With a CoC above 8 deg, the probability of knock combustion with a CTC(2) value reaches less than 40%.

When $\lambda=1.6$, the analysis shows that knock combustion is significantly less probable at CTC = 2. In the prechamber at CTC(2), knock combustion reaches 50% (at CoC = 2 deg aTDC). With an active pre-chamber, knock combustion has the highest probability when the centre of combustion occurs earlier (Fig. 10a). In this case, it is observed that the probability of cycle-by-cycle knock combustion is higher in PC than in MC. This is caused by the fact that a small CoC is achieved by increasing the fuel dose to the pre-chamber.

Figure 10b also shows the above trend. At $\lambda=2.0$, knock combustion in PC is much more likely than in MC. These values are independent of CoC.

At high values of λ (Fig. 10c), knock combustion occurs only in the pre-chamber. In the worst-case scenario, it has a probability of more than 60% (regardless of the following cycles. However, CTC(2) analysis shows that the probability is reduced to 40% (at CoC = 3 deg aTDC).

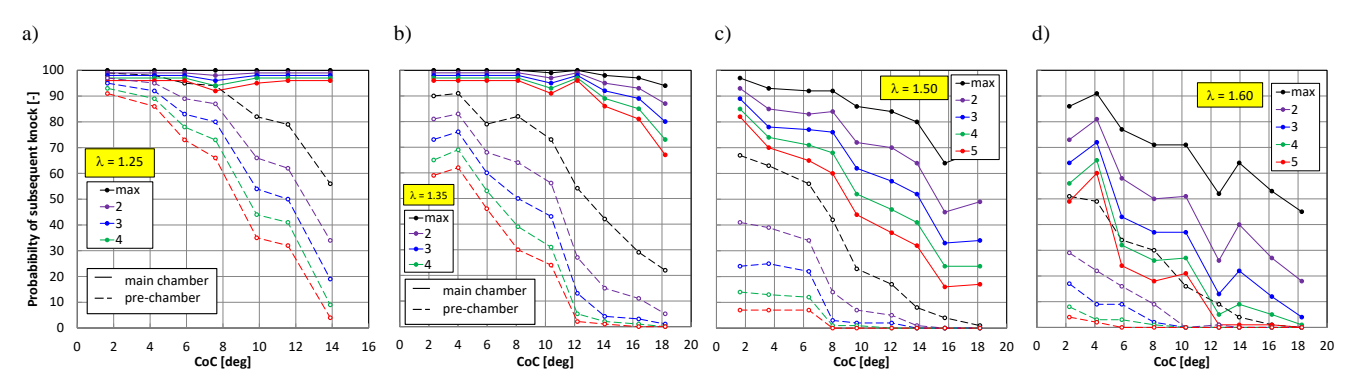


Fig. 9. Probability of two to five subsequent knock cycles at different excess air ratio values (passive pre-chamber): a) at $\lambda = 1.25$, b) at $\lambda = 1.35$, c) at $\lambda = 1.5$, d) at $\lambda = 1.6$

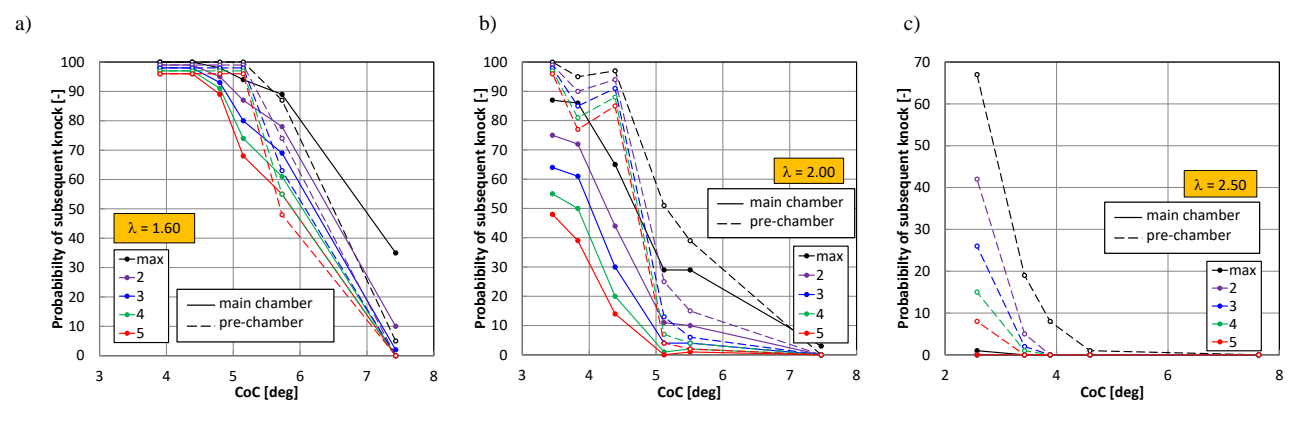


Fig. 10. Probability of two to five subsequent knock cycles at different excess air ratio values (active pre-chamber): a) at $\lambda = 1.6$, b) at $\lambda = 2.0$, c) at $\lambda = 2.5$

4. Conclusions

- 1. During tests with a passive pre-chamber, MAPO is more than 2 times higher in the MC chamber than in the PC. It decreases with an increase in the excess air ratio.
- 2. During tests with the active pre-chamber, the MAPO value reached a similar value in both chambers (for λ = = 1.6). However, for more lean air-fuel mixtures, MAPO in the PC is higher than in the MC. This situation persists until λ = 3.0, after which knock occurs only in the pre-chamber.
- 3. Knock combustion in the passive pre-chamber system occurs when λ reaches low values and remains high up to $\lambda = 1.6$. When $\lambda = 2.0$, knock combustion is strongly limited by the excess air ratio. A significant reduction of knock combustion is possible by delaying the combustion centre (independent of the excess air ratio).

- 4. Knock combustion in the active combustion chamber system occurs up to $\lambda=2.0$; it is more frequent in PC than in MC.
- 5. In the passive pre-chamber system, the probability of knock combustion in 3 consecutive cycles (CTC(3)) is strongly reduced when an increase in λ and does not occur at $\lambda > 3$ and CoC > 8 deg.
- 6. The probability of knock combustion with an active prechamber is higher in the PC than in the MC. Once the CoC > 5 deg aTDC is exceeded, the probability drops rapidly to minimum values regardless of λ.

Acknowledgements

The work was supported by the 'PhDBoost' Program for doctoral students of the Doctoral School of Poznan University of Technology (in 2024) from the University's subsidy financed from the funds of Ministry of Science and Higher Education; and by statutory work: 0415/SBAD/0351 and 0415/SBAD/0353.

Nomenclature

CoCcenter of combustion **MFB** mass fraction burned **CTC** MFM mass flow meter cycle-to-cycle indicated the mean effective pressure PC pre-chamber **IMEP** MAPO maximum amplitude pressure oscillation **TDC** top dead center main chamber MC air excess ratio

Bibliography

- [1] Aramburu A, Guido C, Bares P, Pla B, Napolitano P, Beatrice C. Knock detection in spark ignited heavy duty engines: an application of machine learning techniques with various knock sensor locations. Measurement. 2024;224: 113860. https://doi.org/10.1016/j.measurement.2023.113860
- [2] Aziz M, Wijayanta AT, Nandiyanto ABD. Ammonia as effective hydrogen storage: a review on production, storage and utilization. Energies. 2020;13(12):3062. https://doi.org/10.3390/en13123062
- [3] Brecq G, Bellettre J, Tazerout M. A new indicator for knock detection in gas SI engines. Int J Therm Sci. 2003;42(5): 523-532. https://doi.org/10.1016/S1290-0729(02)00052-2
- [4] Chai WS, Bao Y, Jin P, Tang G, Zhou L. A review on ammonia, ammonia-hydrogen and ammonia-methane fuels. Renew Sustain Energy Rev. 2021;147:111254. https://doi.org/10.1016/j.rser.2021.111254
- [5] Dimitriou P, Javaid R. A review of ammonia as a compression ignition engine fuel. Int J Hydrog Energy. 2020;45(11): 7098-7118. https://doi.org/10.1016/j.ijhydene.2019.12.209
- [6] Górzyńska M, Pielecha I. Numerical investigation of prechamber holes diameter geometry on combustion parameters in a hydrogen-powered Turbulent Jet Ignition engine. Combustion Engines. 2024;199(4):126-139. https://doi.org/10.19206/CE-193950
- [7] Güdden A, Pischinger S, Geiger J, Heuser B, Müther M. An experimental study on methanol as a fuel in large bore high speed engine applications port fuel injected spark ignited combustion. Fuel. 2021;303:121292. https://doi.org/10.1016/j.fuel.2021.121292
- [8] Guo X, Li T, Huang S, Zhou X, Chen R, Wei W et al. Characteristics of ignition, combustion and emission formation of premixed ammonia-hydrogen blends by hydrogen-fueled pre-chamber turbulent jets. Energy. 2025; 322:135573. https://doi.org/10.1016/j.energy.2025.135573

- [9] Gürbüz H, Topalci Ü, Akçay H. Experimental evaluation of the combustion process of H₂-assisted flame jet ignition conditions in a direct injection gasoline SI engine. Appl Therm Eng. 2025;270:126248. https://doi.org/10.1016/j.applthermaleng.2025.126248
- [10] Ji F, Meng S, Han Z, Dong G, Reitz RD. Progress in knock combustion modeling of spark ignition engines. Appl Energy. 2025;378:124852. https://doi.org/10.1016/j.apenergy.2024.124852
- [11] Liu X, Menaca R, Mohan B, Silva M, AlRamadan AS, Cenker E et al. Assessment of piston and injector cap designs on the performance of a hydrogen direct-injection spark-ignition engine. Appl Therm Eng. 2025;271:126372. https://doi.org/10.1016/j.applthermaleng.2025.126372
- [12] Matla J, Kaźmierczak A, Haller P, Trocki M. Hydrogen as a fuel for spark ignition combustion engines – state of knowledge and concept. Combustion Engines. 2024;196(1): 73-79. https://doi.org/10.19206/CE-171541
- [13] Menaa A, Amrouche F, Lounici MS, Loubar K. Experimental investigation of hydrogen use in dual fuel and like dual fuel mode. Fuel. 2025;393:135031. https://doi.org/10.1016/j.fuel.2025.135031
- [14] Pielecha I, Szwajca F, Skobiej K. Experimental investigation on knock characteristics from pre-chamber gas engine fueled by hydrogen. Energies. 2024;17(4):937. https://doi.org/10.3390/en17040937
- [15] Pla B, Bares P, Jimenez I, Guardiola C. Increasing knock detection sensitivity by combining knock sensor signal with a control oriented combustion model. Mech Syst Signal Process. 2022;168:108665. https://doi.org/10.1016/j.ymssp.2021.108665
- [16] Puzinauskas PV. Examination of methods used to characterize engine knock. SAE Technical Paper. 920808. 1992. https://doi.org/10.4271/920808

- [17] Rimkus A, Kozłowski E, Vipartas T, Pukalskas S, Wiśniowski P, Matijošius J. Emission characteristics of hydrogenenriched gasoline under dynamic driving conditions. Energies. 2025;18(5):1190. https://doi.org/10.3390/en18051190
- [18] Shi H, Tang Q, Uddeen K, Magnotti G, Turner J. Optical diagnostics and multi-point pressure sensing on the knocking combustion with multiple spark ignition. Combust Flame. 2022;236:111802. https://doi.org/10.1016/j.combustflame.2021.111802
- [19] Shi W, Li Z, Dong W, Sun P, Yu X, Yang S et al. Effect of pre-combustion chamber hydrogen injection strategy on emissions and fuel economy of jet ignition engines under ultra lean-burn conditions. Int J Hydrog Energy. 2025;113: 147-160. https://doi.org/10.1016/j.ijhydene.2025.02.421
- [20] Silva M, Liu X, Hlaing P, Sanal S, Cenker E, Chang J et al. Computational assessment of effects of throat diameter on combustion and turbulence characteristics in a pre-chamber engine. Appl Therm Eng. 2022;212:118595. https://doi.org/10.1016/j.applthermaleng.2022.118595
- [21] Sun J, Zhang X, Tang Q, Wang Y, Li Y. Knock recognition of knock sensor signal based on wavelet transform and variational mode decomposition algorithm. Energy Convers Manag. 2023;287:117062. https://doi.org/10.1016/j.enconman.2023.117062
- [22] Szwaja S, Naber JD. Dual nature of hydrogen combustion knock. Int J Hydrog Energy. 2013;38(28):12489-12496. https://doi.org/10.1016/j.ijhydene.2013.07.036

Filip Szwajca, DEng. – Faculty of Civil and Transport Engineering, Poznan University of Technology, Poland.

e-mail: filip.szwajca@put.poznan.pl



- [23] Verhelst S, Wallner T. Hydrogen-fueled internal combustion engines. Prog Energy Combust Sci. 2009;35(6):490-527. https://doi.org/10.1016/j.pecs.2009.08.001
- [24] Wakasugi T, Tsuru D, Tashima H. Influences of the prechamber orifices on the combustion behavior in a constant volume chamber simulating pre-chamber type mediumspeed gas engines. Combust Engines. 2022; https://doi.org/10.19206/CE-148171
- [25] Wang K-D, Zhang Z-F, Sun B-G, Zhang S-W, Lai F-Y, Ma N et al. Experimental investigation of the working boundary limited by abnormal combustion and the combustion characteristics of a turbocharged direct injection hydrogen engine. Energy Convers Manag. 2024;299:117861. https://doi.org/10.1016/j.enconman.2023.117861
- [26] Yang X, Li G, Liang Y, Wang P, Cheng Y, Zhao Y. Effect of auxiliary hydrogen injection in the prechamber on the combustion process of a natural gas engine. ACS Omega. 2025;10(12):11935-11947. https://doi.org/10.1021/acsomega.4c08779
- [27] Zhu S, Akehurst S, Lewis A, Yuan H. A review of the prechamber ignition system applied on future low-carbon spark ignition engines. Renew Sustain Energy Rev. 2022;154: 111872. https://doi.org/10.1016/j.rser.2021.111872
- [28] Zuo Q, Yang D, Shen Z, Chen W, Lu C, Chen L et al. Effect of premixed ratio on combustion and emission characteristics in a spark ignition engine with hydrogen-ammonia direct injection. Fuel. 2025;393:135051. https://doi.org/10.1016/j.fuel.2025.135051

Prof. Ireneusz Pielecha, DSc., DEng. – Faculty of Civil and Transport Engineering, Poznan University of Technology, Poland.

e-mail: ireneusz.pielecha@put.poznan.pl



Dawid Mielcarzewicz, MEng. – Faculty of Civil and Transport Engineering, Poznan University of Technology, Poland.

e-mail:

dawid.miel carzewicz@doctorate.put.poznan.pl

